

Electrical Machines Fault Detection through Frequency Response Analysis (FRA) - Part I: Stator*

Reza Khalilisenobari⁺ and Javad Sadeh[×]

Electrical Engineering Department, Faculty of Engineering, Ferdowsi University of Mashhad, Mashhad, Iran

Abstract

Remarkable performance of the Frequency Response Analysis (FRA) technique in transformers' fault detection, structural similarity between transformers and electrical machines, and the importance of machines' condition monitoring are the main reasons for studying FRA in the electrical machines. In this paper, the application of the FRA method for electrical machines fault detection is investigated by experimental tests on a three-phase wound-rotor asynchronous machine. First, the effect of the rotor position on the sound and defective stator frequency responses is assessed under different circuit connections. Second, the applicability of the FRA for detection of the stator inter-turn and phase to phase short-circuit faults and insulation weaknesses is evaluated by considering fault resistance, location, and severity. Third, the best circuit connection for fault detection is determined. Finally, the performance of a wide range of statistical indices that are used for FRA results comparison is studied to find the best one. A new index for FRA interpretation is also introduced.

Keywords: Frequency response analysis (FRA), electrical machines, fault detection, condition monitoring

1. Introduction

Electrical machines are undeniably the most critical part of the power system. The generators supply a large portion of the electrical energy, and on the consumption side, electrical motors have indisputable roles primarily in the industrial section. Therefore, the precise, efficient, and continuous performance of electrical machines is necessary for having a sustainable industrial development and reliable power system. Additionally, the high economic value of these devices adds to their importance. So, it is crucial to monitor their condition continually and detect their faults and failures in the incipient stages. Initially, simple protection schemes were used to ensure the integrity and safe operation of machines. As the application of electrical machines became widespread, improvements are made in the field of condition monitoring and fault detection, and it is also developing [1].

Frequency Response Analysis (FRA) is a comparison-based method for electrical apparatus condition assessment, which was firstly introduced by Dick and Erven for transformers' fault detection in 1978 [2]. Since then, many research works are done in the field of transformers' FRA that we had entirely reviewed in [3]. Based on that paper, general classification and description of the literature in the transformers' FRA are brought here to understand the current state-of-art in electrical machines' FRA.

Literature in the transformers' fault detection through FRA can be categorized into three levels. In the first place, most of the investigations were focused on the effect of faults and failures and non-error parameters on the FRA results [4-7]. By this researches, the applicability of the FRA method for transformers' fault detection is evaluated. Also, essential issues and considerations for FRA practice are revealed. Thus, users, as well as researchers, became more familiar with FRA performance in different conditions and failures. These studies are the basis of the FRA application in transformers and paved the way for further inquiries and better interpretation of the results. In the second level, researchers tried to enhance the interpretation routine of the FRA results by analyzing comparison methods and studying statistical indices that can be used for comparing FRA results [8,9]. Some research works also tried to compensate for FRA weaknesses by the collaboration of other methods [10,11]. The ultimate level of investigations in the field of transformers' FRA contains the works that try to eliminate or minimize the human interference in the interpretation of FRA results and developed automated fault detection algorithms [12-15]. This group of works mainly relies on developing models for transformers and validating them with experimental results. Thus, it is possible to perform simulations on these models for better understanding the characteristics of the FRA responses. As a result of these different levels of investigations, FRA is currently known as one of the most reliable fault detection techniques, and organizations such as IEC, IEEE, and CIGRE standardized it as a routine test for transformers [16-18].

* This paper is a preprint of a paper submitted to IET Electric Power Applications. If accepted, the copy of record will be available at the IET Digital Library

⁺ Reza Khalilisenobari was with the Department of Electrical Engineering, Ferdowsi University of Mashhad, Mashhad, Iran. Currently, he is with School of Electrical, Computer and Energy Engineering, Arizona State University, Tempe, AZ, U.S. E-mail address: rezakhalili@asu.edu

[×] Corresponding author at: Electrical Engineering Department, Faculty of Engineering, Ferdowsi University of Mashhad, P.O. Box: 917775-1111, Mashhad, Iran. Tel.: +98 513 8763302; fax: +98 513 8763302. E-mail address: sadeh@um.ac.ir (J. Sadeh).

On the one hand, the FRA fault diagnosis technique has a significant performance in transformers. On the other hand, it is always crucial to develop more precise condition monitoring methods for electrical machines, and they are very close in structure to the transformers. Therefore, FRA recently is used as a fault detection method for electrical machines, and it is in its first steps of development. Due to the novelty of the FRA method for electrical machines, a few numbers of research are done in this field. Like the first level of investigation in the transformers, most of the current inquiries deal with the applicability evaluation of this method in electrical machines by performing FRA experiments. In addition to applicability evaluation, the practical tests' results familiarize the experts with the effect of various parameters on the FRA results and also provide a footstone for further investigations in result interpretation and model development.

Investigations show that FRA can detect interlayer short-circuits in a single coil of a winding, so, it can be used as a quality control technique in the manufacturing process of the electrical machines [19,20]. Additionally, it is illustrated that FRA can detect stator problems of squirrel cage asynchronous machines [20-22] or synchronous ones [23]. FRA can also evaluate the condition of stator insulations [24-26]. Examinations showed that change in the position of the rotor may have effects on the stator's FRA results and can challenge the fault detection procedure, but an appropriate solution for addressing this issue is also suggested [23,27,28]. Finally, the applicability of FRA for synchronous machine's rotor fault detection is analyzed in [28] and, reference [29] tried to expand the research in this field to the level of interpretation improvement by introducing a trend-based comparison method. These investigations do not consider some issues like the difference in the accuracy of various circuit connections for FRA tests, the effect of rotor position in faulty conditions, and do not fortify their analyses by mathematical methods.

Apart from the abovementioned shortcomings, these works are essential and basis for FRA studies in the electrical machines. Subsequently, further researches must be done to cover the gap of previous works and also study topics like three-phase rotor fault diagnosis or wound rotor asynchronous machines fault detection. Also, the same as the trend of research works in transformers, investigations in this field must deal with issues related to the interpretation level of the FRA results to have FRA as an efficient fault detection procedure for electrical machines.

In this paper, the topic of electrical machines stator's fault detection with FRA is thoroughly studied. The main contributions of this work are as follows:

- All the analyses of this work are done on a wound rotor asynchronous machine due to two main reasons: First, this type of machine has a wide range of applications in power generation and large-scale industrial units. Second, having access to the rotor's terminal in this machine provides the opportunity for investigating a wide range of topics in the field of electrical machines' FRA. Despite the importance and advantage of this type of machine, to the best of our knowledge, FRA on wound rotor asynchronous machine has not been investigated before.
- The effect of the rotor's position on the frequency responses of the stator in different terminal connections of the rotor is examined. Additionally, for the first time, the rotor's position influence in faulty conditions is investigated to have more insight on this issue. Finally, fault detection accuracy in different rotor's terminal connections is compared, and the best connection type is chosen.
- To evaluate FRA performance, FRA results in various fault locations, and resistances of stator's inter-turn and phase to phase short-circuit faults are presented besides FRA results in stator's insulation weakness conditions. In contrast to other papers, figures in this paper are compared with each other by absolute average difference (DABS) index that had shown decent performance in the interpretation of transformers' FRA results [8].
- Statistical indices are fundamental for achieving the goal of standardizing and automating fault detection procedure with FRA. On the one side, they can be used besides visual comparison of results to enhance accuracy. On the other side, they are crucial for feature extraction in algorithmic fault detection techniques. In the last part of the paper, more than twenty statistical indices are examined over practical results; to study their features. More importantly, a new index is introduced in this paper that has better performance in comparison to the existing ones.

The remainder of this paper is organized as follows. Section 2 briefly describes FRA principles and the experimental setup of this work. Section 3 presents and paraphrases the experimental tests results in different subsections, and statistical comparison methods are analyzed in Section 4, along with the introduction of a new index. Finally, Section 5 draws relevant conclusions. Issues related to the rotor fault detection is investigated in the latter part of this series of papers to thoroughly study the topic of the electrical machines fault detection through FRA.

2. Frequency Response Analysis Principle and Test Practice

FRA is a non-invasive and non-destructive test that is based on measuring windings response in a wide frequency range. The responses which are in the form of transfer functions are directly related to the RLC network of the under-test device. Geometry and construction of the windings are the parameters that determine the

apparatus's RLC network, so, any changes in the windings can affect the RLC network and also the frequency responses. Consequently, comparing the actual FRA test result with reference response (signature or fingerprint) which is measured when the device is sound could reveal changes in the machine or transformer's condition and results in fault diagnosis [3].

For measuring the frequency response, a sweep frequency or impulse signal is injected into one of the winding's terminals which is called the input signal. Then, the output signal is measured in any other terminals of the device according to the measurement type. Subsequently, the frequency response magnitude and phase angles are calculated using input and output signals with respect to the intended transfer function. Due to the comparative nature of the FRA method, the type of the used transfer function does not affect the test principle; while it may cause changes in the quality of the FRA results. For example, different transfer functions may have different accuracies in fault detection. Generally, the frequency response can be measured as a voltage ratio of two terminals or as an input impedance or admittance of a winding [3]. Input impedance is the used transfer function for the tests of this paper.

In this work, Wayne Kerr Electronics 6530B impedance analyzer is used for conducting FRA tests and measuring the winding's impedance in a wide frequency range. This equipment measures impedance (Z) and phase angle (θ) as well as some other parameters in the 20 Hz to 30 MHz frequency range with a $\pm 0.05\%$ error.

The FRA tests of this research are performed on a 4.5^{kW} , $220/380^V$ three-phase wound-rotor asynchronous machine to investigate different issues in this field. Windings of this machine are rewound to extract five terminals on different locations of the stator windings (terminals AI, BI, BII, BIII, and CI in Fig. 1) and three terminals on the rotor windings (terminals xi, xii, and n in Fig. 1). These terminals are separate from the standard terminals of this kind of machine (terminals Aa, Ab, Ba, Bb, Ca, Cb, x, y, and z in Fig.1) and are used for modeling faults. Fig. 1 demonstrates the machine's windings map and the exact position of the terminals. Fig. 2 shows the whole test setup of this work.

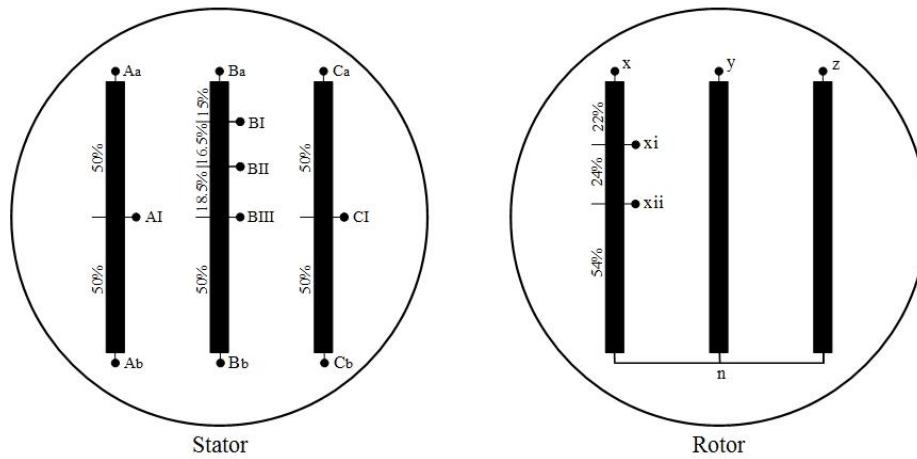


Fig. 1: Winding map of the machine used in this research

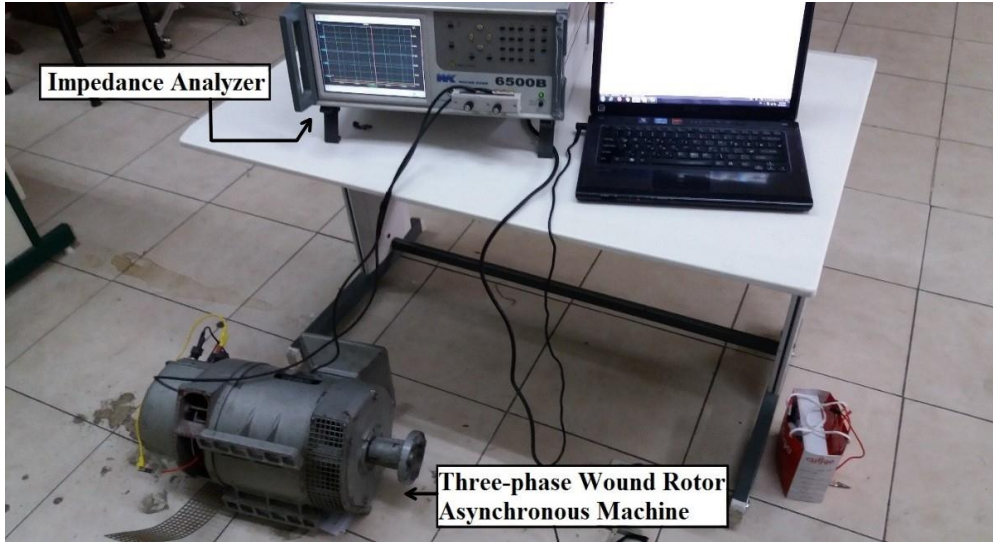


Fig. 2: Test setup

3. Investigation of the Issues Related to the Stator Fault Detection

More than fifty FRA tests are performed on the machine's stator in different situations to study various topics related to stator fault detection using FRA. Due to the initial analysis of the frequency range adequacy, the frequency range of tests is chosen to be 20 Hz to 5 MHz. Also, it is crucial to be ensured that FRA tests are repeatable, which means that repeated tests in the same conditions must have identical results, and only FRA responses change when test procedure varies, or faults happen on the device. Therefore, the repeatability of the tests is ensured by performing the same test several times and getting similar results. Similar results mean that there may be some differences between them, but differences are very minute and are not interpreted as faults. *DABS* index is calculated two by two between the test results that are done for checking repeatability to have a reference for the acceptable difference between test results in the same conditions. The average of those calculated indices is respectively 4.29 Ω and 0.84° for amplitude and phase angle diagrams. These values are referred to as no-fault *DABS* values in the remainder of the paper. Note that *DABS* index is calculated by equation (1), where x_i are the data points of the reference curve, y_i are the data points of the current FRA curve, and N is the total number of data points. The index value is zero when compared curves are completely identical. In the following, the results of FRA tests are presented and paraphrased in their related subsection.

$$DABS = \frac{1}{N} \sum_{i=1}^N |x_i - y_i| \quad (1)$$

3.1. Effect of Rotor Position on the FRA Results of Stator Windings

Existence of the rotor as a moving part in the electrical machines is one of the main differences between transformers and rotating machines from the FRA perspective. Analyzing the rotor's influence on the stator's FRA result is a topic that gained the researcher's attention from the beginning. Change in the rotor position may affect the results and can cause errors in the fault diagnosis procedure. Therefore, the effect of the cylindrical wound three-phase rotor's position on the FRA results is presented in this section. To the best of our knowledge, the effect of this type of rotor is not analyzed in previous works.

In order to deal with this issue, the frequency response of the stator's phase B (impedance from Ba and Bb terminals of Fig. 1) is measured in six different positions of the rotor for two different conditions of rotor's terminal connections (short-circuit and open circuit). Fig. 3 shows the FRA results when the rotor's terminals are floated, and Fig. 4 illustrates the results in the short-circuit condition of terminals. Note that the machine's stator is sound, and no fault is modeled on it in these two figures.

It must be mentioned that if assume the POS. 1 as a reference, POS. 2 to POS. 6 are respectively 80, 130, 180, 270 and 320 degrees clockwise ahead from the reference. These positions are chosen erratically to avoid the effect of similarity and symmetry in the rotor's structure.

For a better understanding of the rotor's influence on FRA results, the frequency response of the stator is also measured in different positions of the rotor when there is an inter-turn fault on the stator's winding. FRA results of the stator's phase B in various rotor positions when there is a solid short-circuit fault between BI and BII

terminals (Fig. 1) are demonstrated in Figs. 5 and 6. In Fig. 5, rotor terminals are floated, and in Fig. 6, they are short-circuited.

To have an accurate analysis of the presented results, in each figure the difference between POS. 1 curve and other curves is calculated using the *DABS* index. Then the average of the calculated indices for each figure is brought in Table 1.

Table 1: Average of *DABS* index for comparing curves in Fig. 3 to Fig.6

Compared Curves	Fig. 3	Fig. 4	Fig. 5	Fig. 6
Average of <i>DABS</i> for Amplitude diagram	16.67	6.88	13.41	7.45
Average of <i>DABS</i> for Phase Angle diagram	0.45	1.83	0.5	1.59

According to Figs. 3 to 6 and Table 1, it is evident that changes in the rotor position affect the FRA results, although the rotor of this machine is cylindrical and completely symmetric. This issue can cause a problem in fault detection and must be considered in the test routine. Additionally, in both faulty and sound conditions, FRA results are more severely affected when rotor terminals are floated. For example, according to Table 1, the average value of the *DABS* index in Fig. 3 is fourfold of No-Fault *DABS* value (4.29). Additionally, short-circuiting rotor terminals mitigate the effect of the rotor's position on the amplitude diagram of the stator's frequency responses in a way that it is possible to ignore the changes of the results. Despite that, the phase angle diagrams have more changes in this circuit connection comparing to the condition that terminals are floated. Note that although stator's FRA results are more sensitive to the change of rotor position when rotor terminals are floated, this sensitivity can be interpreted as the higher accuracy of this type of connection. This topic is discussed in the following sections.

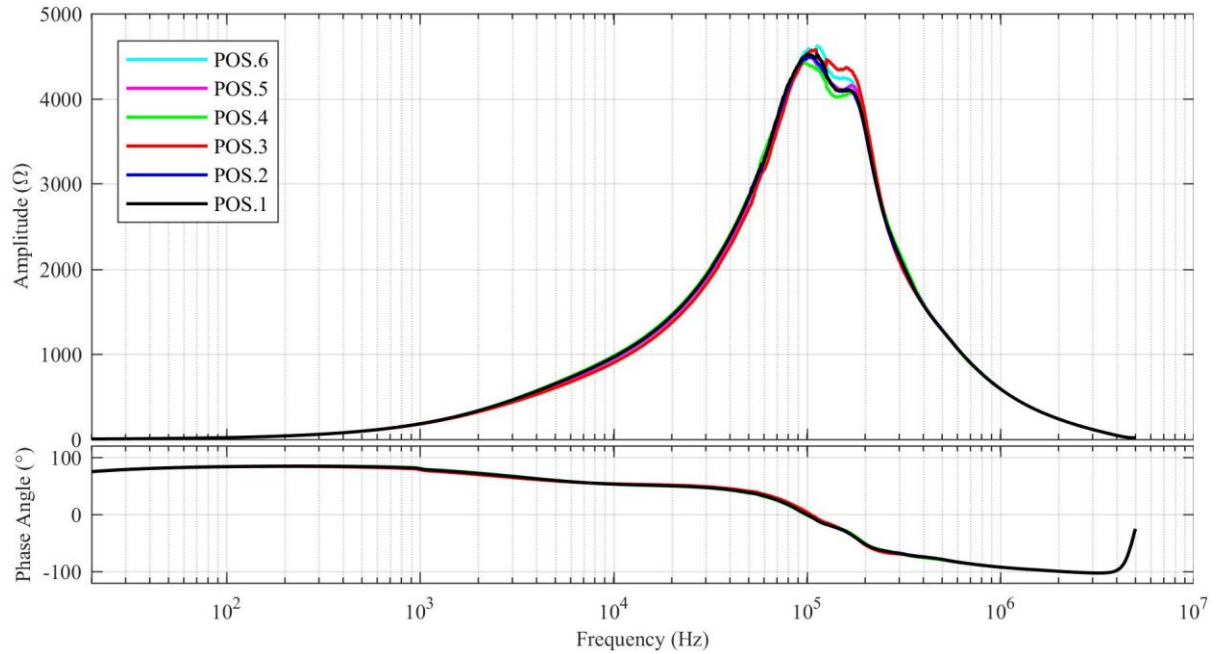


Fig. 3: Stator's phase B frequency response in various rotor positions (rotor's terminals are floated)

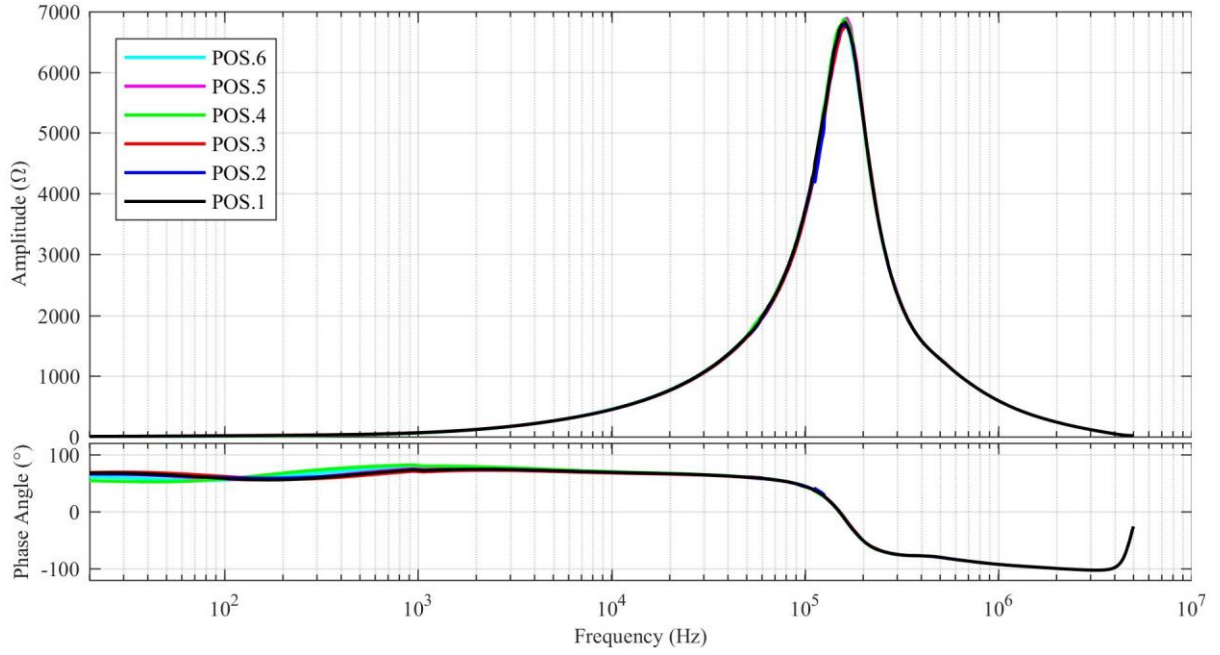


Fig. 4: Stator's phase B frequency response in various rotor positions (rotor's terminals are short-circuited)

In the faulty cases (Figs. 5 and 6), the shapes of responses are different from Figs. 3 and 4 as a result of inter-turn fault existence; but it is important to pay attention to the way that curves of each figure vary from each other due to the rotor position changes. For instance, in Fig. 3, curves are too close to each other in frequencies higher than 200 kHz, but in faulty condition (Fig. 5), there is an apparent dissimilarity in the 200 kHz to 500 kHz frequency range just because of change in the rotor position. Furthermore, the curves of Fig. 3 are more disperse from each other than the curves of Fig. 5 in the lower frequency range (1 kHz to 70 kHz). Consequently, due to the fault-caused asymmetry of the stator, changes of the rotor position may result in additional variations in the responses, and this issue can harden fault detection procedure or cause fault's severity misinterpretation. Similar to the previous works that have analyzed the rotor' position influence on the frequency response of stator [23,27,28], the results of analyses mentioned above also recommend that the rotor position must be constant in all of the FRA tests to avoid any mistakes. It is also considered in all of the later experiments of this paper.

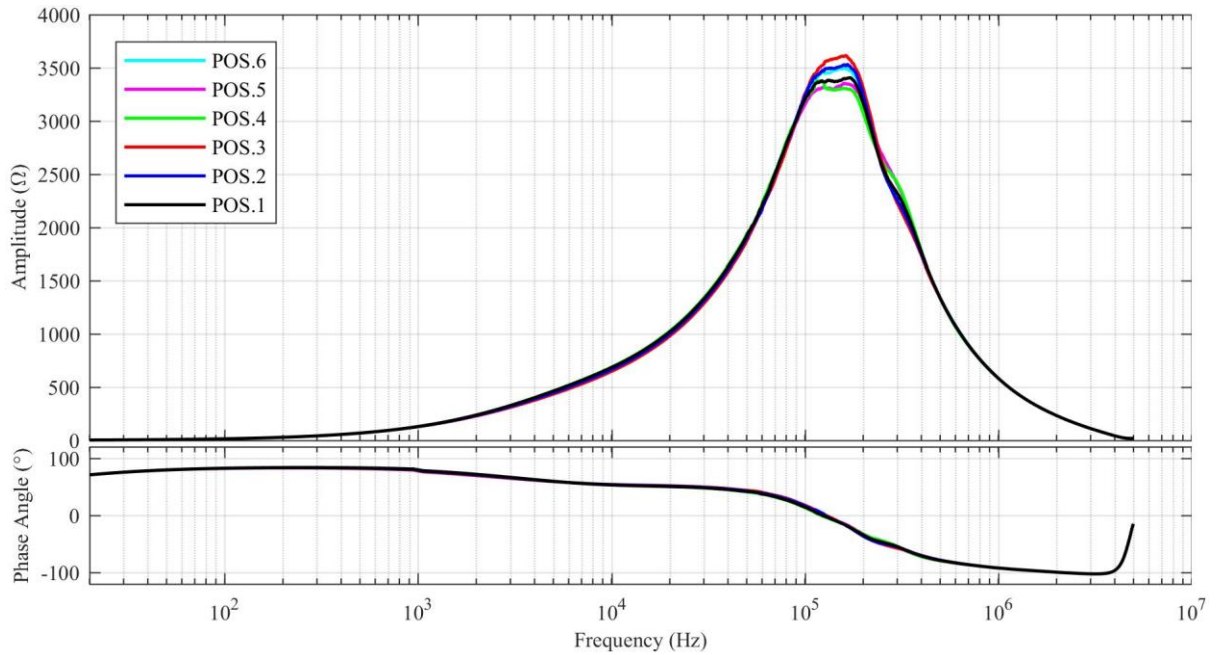


Fig. 5: Stator's phase B frequency response in faulty condition and various rotor positions (rotor's terminals are floated)

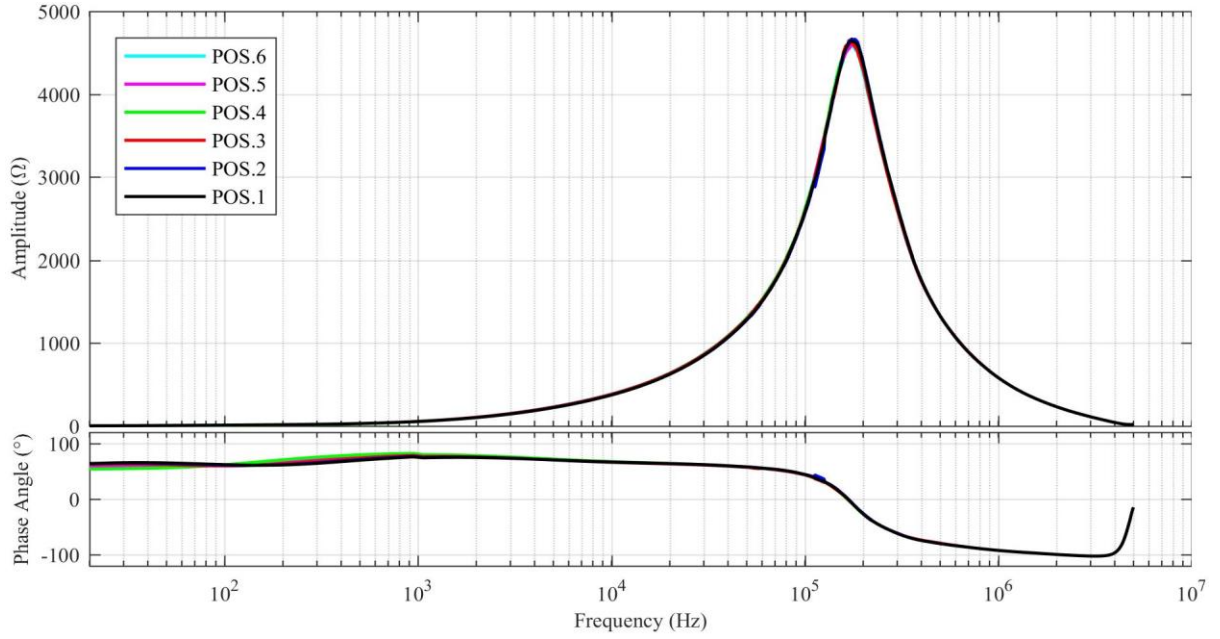


Fig. 6: Stator's phase B frequency response in faulty state and different rotor positions (rotor's terminals are short circuit)

3.2. Evaluation of Stator's FRA Test Accuracy in Different Connections of Rotor Terminals

In the wound-rotor machines, it is possible to measure the frequency response of the stator when rotor terminals are short-circuited, or they are floated. In this section, it is analyzed that in which condition the FRA results have better accuracy for finding stator's faults. The frequency response of the stator's phase B is measured in sound condition when the rotor's terminals are short-circuited, and when they are floated. Additionally, the FRA test is also performed in these two connections when inter-turn short-circuit fault is modeled between BI and BII taps. The results of these four tests are presented in Fig. 7.

In Fig. 7, the difference between the faulty and reference amplitude curves of the open circuit rotor test (red and black) is apparent from 1 kHz up to about 500 kHz, but results of the short-circuit rotor tests (green and blue) separated from each other in a decade later (10 kHz). Additionally, the difference between amplitude diagrams of the green and blue curves is more than the difference of the curves in the floated connection type. It seems hard to choose the best connection type by visual analysis. Thus, the curves of each connection type are compared with each other by the *DABS* index. The index value is 226.12 Ω for black and red curves (open circuit rotor) and 182.57 Ω for blue and green charts (short-circuit rotor), and the calculated *DABS* index for phase angle diagrams is respectively 2.81° and 3.36° for float and short-circuit connections. As it is usual to use amplitude diagrams for fault detection, it can be concluded from the results that FRA tests are more accurate for fault detection when rotor terminals are floated. It must be mentioned that several tests are also performed to study the rotor's connection effect on the FRA accuracy in other types of faults like phase to phase one. These tests also showed that the faults are more apparent when the rotor's terminals are floated. The results of these tests are not presented to avoid prolongation.

Note that in a wide range of electrical machines, rotor terminals are not accessible, or there are short-circuited (squirrel rotors). So, in these cases, it is impossible to perform the FRA test in an open circuit rotor condition. Subsequently, although the results show that it is better to do the FRA test when rotor terminals are floated, and authors also recommend this connection for practice, if applicable; The other tests of this paper are done on short-circuited rotor situation to have conclusions that are valid for all types of machines.

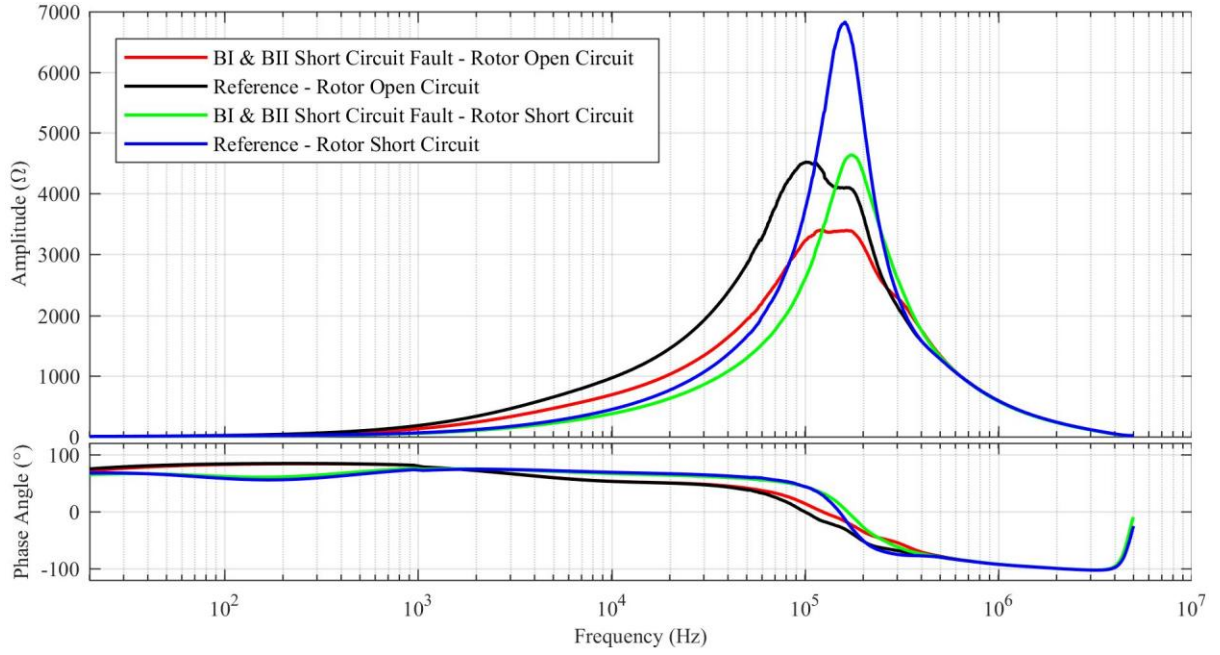


Fig. 7: Comparison of FRA tests accuracy in different connections of rotor's terminals

3.3. Performance of the FRA Test in Detection of Various Stator's Faults

In this section, FRA test performance for diagnosis of inter-turn short-circuit fault, phase to phase short-circuit fault, and isolation failure is evaluated by modeling them on the stator with various severities and also in different locations. Furthermore, this section's results can show how the FRA test can be affected by various faults.

First of all, the inter-turn short-circuit fault is investigated. For doing that, the stator's phase B impedance is acquired when rotor terminals are short-circuited, and inter-turn faults are applied on different taps of the stator. Fig. 8 shows the results of these tests.

Green, purple, red, blue, and cyan are the order of the curves in Fig. 8 from the least severe fault to the most severe one. These faults respectively short-circuit 15%, 16.5%, 18.5%, 35% and 50% of phase B. The curve of each fault level is also compared with the reference curve using *DABS* index, and calculated values for amplitude and phase angle diagrams are brought along with the fault severity in Table 2.

Table 2: Comparison of Fig. 8 curves with the reference one

Curves that are compared with the reference (black)	Green	Purple	Red	Blue	Cyan
Fault severity (short-circuited portion of winding)	15%	16.5%	18.5%	35%	50%
<i>DABS</i> value for Amplitude diagram	180.81	182.57	238.74	282.52	357
<i>DABS</i> value for Phase Angle diagram	3.65	3.36	5.1	6.18	6.32

Fig. 8 shows that the FRA method is entirely able to detect inter-turn short-circuit faults, and faulty curves are easily recognizable from each other and from the reference response. To better evaluate this fault detection procedure, consider green and purple curves. Although the severities of these two faults are very close to each other and only three more turns of the winding are short-circuited in the purple curve comparing to the green one; the amplitude curves of them are separate from each other and cannot be mistaken. Thus, according to these test results, the FRA method can detect inter-turn faults even if they are small.

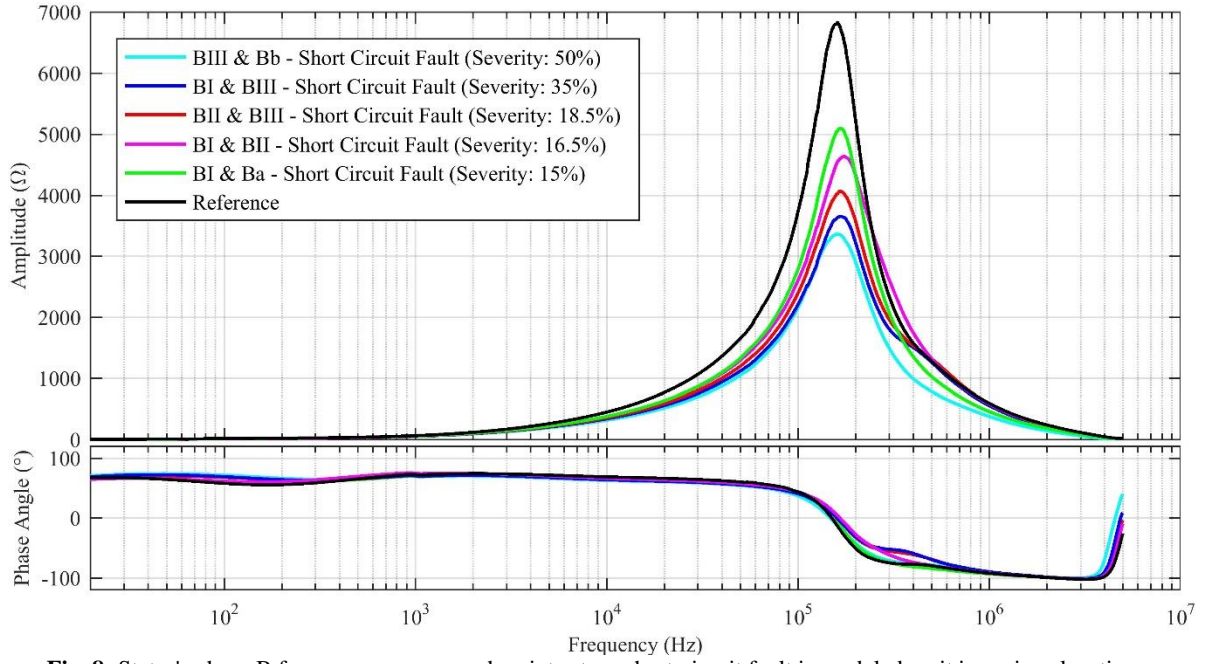


Fig. 8: Stator's phase B frequency response when inter-turn short-circuit fault is modeled on it in various locations

The difference of each curve's amplitude with the reference (black curve) in Fig. 8 is entirely relative to the fault severity, which means that the curve of the most severe fault (cyan) is the farthest curve to the black diagram, and green curve (least severe fault) is the closest curve to the black one. All of the other curves are placed between these two curves according to their fault severity level. The calculated *DABS* values also emphasize this issue. As the fault becomes severe, the *DABS* value rises. Consequently, FRA is not only able to detect these faults, but it can also be used for determining the fault severity.

In Fig. 9, FRA results of phase B are shown in a condition that inter-turn short-circuit fault is modeled between BI and BII taps with different resistances for better assessment of FRA method. As it was expected, the curves of different fault resistances are very close to each other, and part of the diagram is magnified to analyze it better.

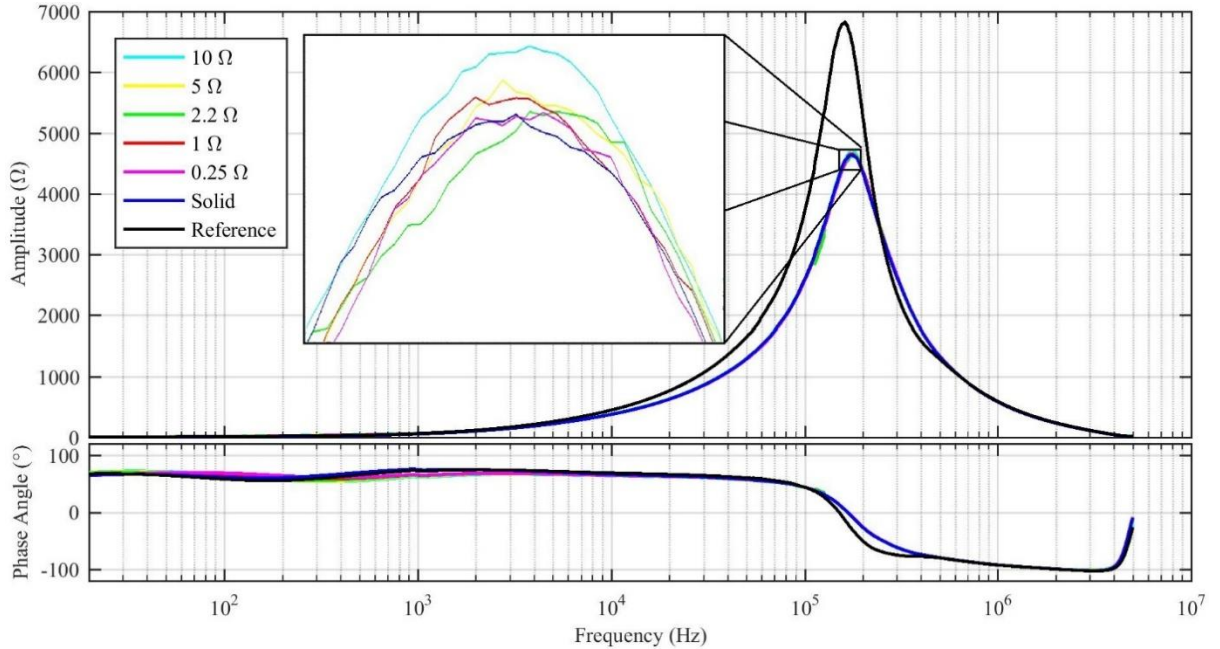


Fig. 9: Stator's phase B frequency response when inter-turn short-circuit fault is modeled on it with different fault resistances

According to the magnified part of Fig. 9, curves of the various fault resistances are distinct from each other, and they are also positioned in relevance to the fault resistance. It means that the purple curve, which is the FRA result of an inter-turn fault with 0.25 Ω resistance, is closest to the zero resistance fault (blue curve). Other curves' position is also relative to their fault resistance, so, the cyan curve (10 Ω fault resistance) is farthest from blue. On

the other hand, the phase angles diagram shows that changes in the resistance of inter-turn fault affect the lower frequency range of the results. Overall, these results emphasize the FRA method accuracy for detecting inter-turn short-circuit faults of the stator that can be considered as an advantage for this method in comparison to other fault diagnosis routines.

The same procedure is taken to assess the FRA method for the diagnosis of phase to phase short-circuit fault. Firstly, the frequency responses are acquired when phase to phase faults are modeled between various taps of the stator's phases A and B, and the results are shown in Fig. 10.

Note that phase to phase fault on the stator cannot be detected by measuring the impedance of each phase (impedance seen by terminals of each winding) when other terminals of the stator are floated. Therefore, for detecting phase to phase faults, the impedance must be measured when phases are two by two series-connected. A comparison of these results with FRA results when the machine is sound can reveal the existence of phase to phase fault. It must be considered that inter-turn fault affects both of the series-connected and solo phases measured impedances, but phase to phase fault just affects the measurement from two by two series-connected phases. Thus, they will not be mistaken with each other.

Measured impedance from Aa and Ba terminals, while Ab is connected to Bb in various phase to phase faults and no-fault (reference) conditions are illustrated in Fig. 10. Each curve of this figure is also compared with the reference curve using the *DABS* index, and the results are presented in Table 3.

Table 3: Comparison of Fig. 10 curves with the reference one

Curves that are compared with reference (black)	Red	Blue	Green
<i>DABS</i> value for Amplitude diagram	568.99	444.88	374.92
<i>DABS</i> value for Phase Angle diagram	12.3	9.51	6.38

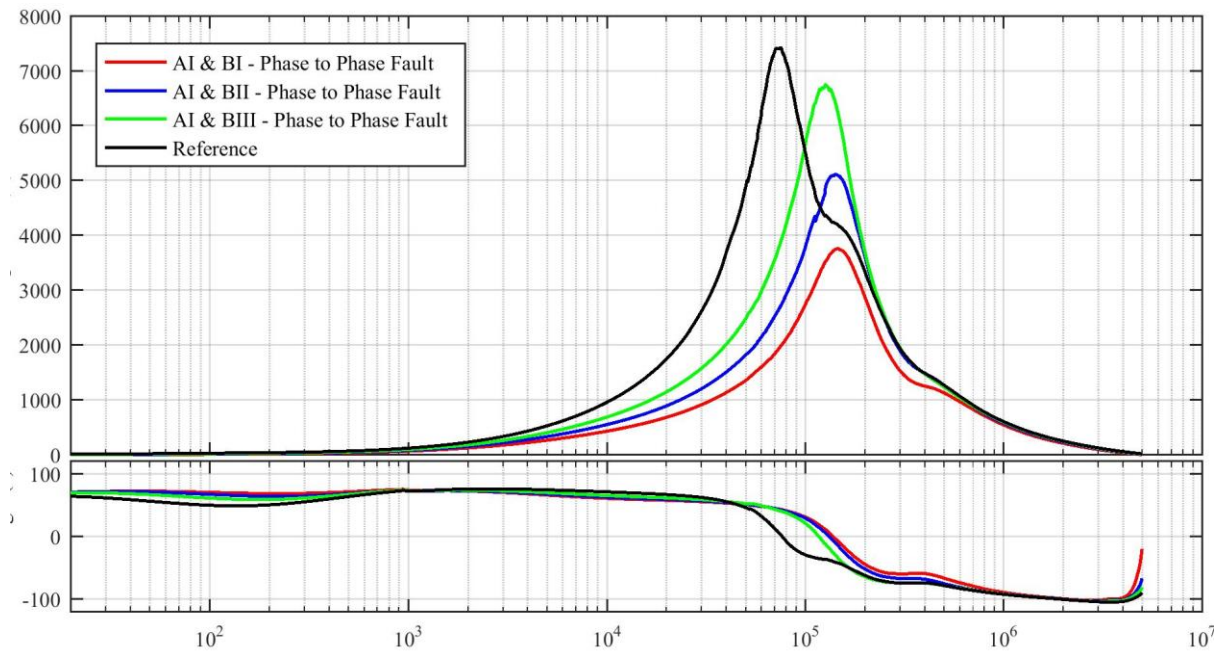


Fig. 10: Series connected phase A and B frequency response when phase to phase fault is modeled between them

Fig. 10 and Table 3 show that the phase to phase fault is entirely apparent in the FRA results. In Fig. 10, the red curve is the farthest curve to the reference, and the green curve is the closest one. It is compliant with the fact that fault between nodes BI and AI (red curve) short-circuits more significant portion of the measured impedance in comparison to the phase to phase fault between BII and AI (blue curve) or BIII and AI (green curve), so, FRA results are rational. In this fault, in contrast to the inter-turn fault, the existence of fault in different locations not only causes a magnitude difference between faulty and reference curves but also leads to a frequency shift in faulty curves in comparison to the reference result. Usually, changes in the test conditions, like rotor position changes, result in magnitude variation of results. So, the frequency shift can enhance fault detection accuracy and also is useful for discriminating inter-turn fault from phase to phase one. As the last row of Table 3 shows and also can be seen in Fig. 10, this fault has a severe effect on the phase angle diagram, in such a way that curves have variations from reference all over the frequency domain. Therefore, using a phase angle diagram besides magnitude curves can enhance fault detection accuracy.

The phase to phase fault detection precision is also challenged by modeling different fault resistances between AI and BIII taps. Fig. 11 shows the resulted curves which are magnified for better illustration. Due to these results,

FRA can separate different fault resistances from each other with acceptable resolution. Curves' order almost follows fault resistance changes, which means faults with higher resistance are above others. Similar to the inter-turn fault, phase angle diagram undergo changes in low-frequency range when fault resistance varies. Overall, the FRA method is capable of detecting phase to phase faults with high sensitivity.

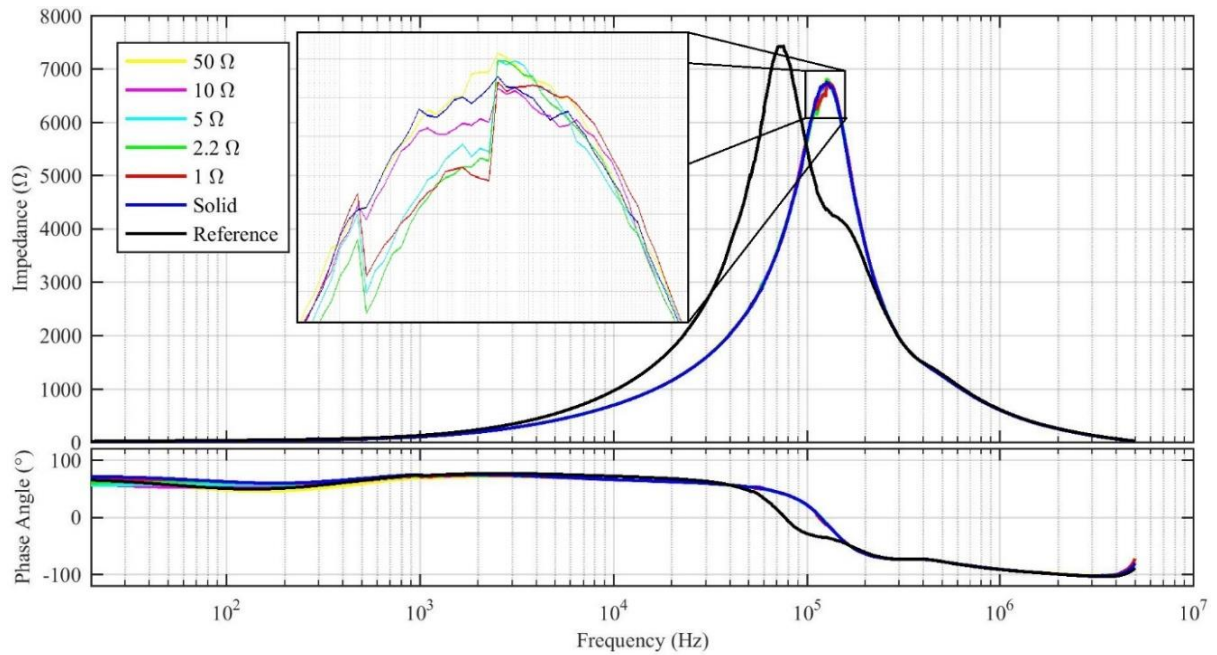


Fig. 11: Series connected phase A and B frequency response when phase to phase fault is modeled between them with different fault resistances

Finally, the FRA test applicability for winding insulation failure is analyzed. Note that the capacitance between insulation layers of the winding increases due to the insulation aging and degradation. Accordingly, it is possible to model insulation weakness by placing capacitors between winding taps and evaluate FRA performance in the detection of this failure [24].

Phase B impedance is measured several times while 100pF , 272pF , 1nF , 10nF , and 100nF capacitors are connected between BI and BII terminals, and resulted curves are brought with a reference curve in Fig. 12. Worth to mention that the rotor position in all of the tests is the same, and it is short-circuited.

Table 4: Comparison of Fig. 12 curves with the reference one

Curves that are compared with the reference (black)	Purple	Blue	Red	Green	Cyan
DABS value for Amplitude diagram	8.91	18.71	58.72	167.03	186.04
DABS value for Phase Angle diagram	3.41	3.51	4.1	6.13	6.66

The least severe insulation weakness is the purple curve, which is quite the same as the reference, and its *DABS* value is also close to the No-Fault *DABS* value ($4.29\ \Omega$). As the capacitors' capacity increases (i.e., the insulation becomes weaker), curves diverge more from the black one. Curves' distance from the reference is proportional to the severity of the modeled insulation weakness. So, FRA is able to assess winding insulation quality. Table 4 and Fig. 12 show that the phase angle diagram is affected all over the frequency range due to insulation weakness. This issue not only can be useful for more accurate insulation condition assessment, but also can cause better discrimination between FRA result of an inter-turn fault, which more affect phase diagram on low and high-frequency parts, and an insulation defect.

Presented test results demonstrate that the FRA method is capable of assessing stator's winding condition and can accurately detect various faults and failures. This section's graphs show the general features of the stator's FRA test results and the pattern that they may be affected due to different failures. Additionally, the effect of non-error conditions like rotor position changes on the results, and the test accuracy in various circuit connections of the rotor was also analyzed in this section. The next section tries to use these FRA results for evaluating mathematical comparison methods and improving FRA interpretation.

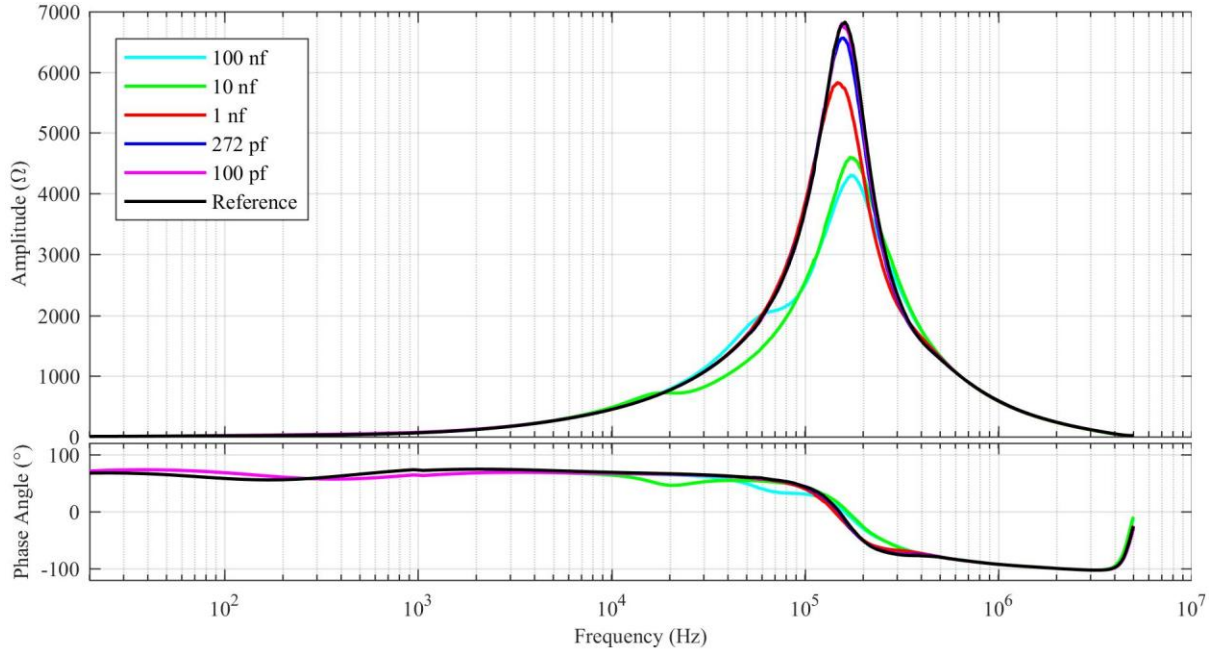


Fig. 12: Stator's phase B frequency response when insulation weakness with different severity is modeled on it

4. Evaluation of Statistical Indices Performance for FRA Interpretation

In this section, twenty-two statistical indices are applied to the experimental results to find the most accurate, sensitive ones. Also, the pros and cons of each index are mentioned to be used in the related application in FRA. This number of indices are not compared in any other FRA studies either on transformers or machines. This comprehensive comparison introduces a reference for the use of indices and also paves the way for FRA interpretation studies in the future. Additionally, based on the observation of this section, a new index is introduced for the FRA result comparison.

Understudy statistical indices can be categorized into two groups: First, one-array indices that are calculated with one set of data (reference curve or actual curve). So, for comparing the curves with this type of indices, the index must be calculated for each curve separately, then, the difference between these two calculated indices shows if curves are the same or not. Second, two-array indices, which use both data arrays simultaneously for calculation of the index. The value of these indices represents the difference between curves. The average index is one of the well-known one-array indices, and the correlation coefficient is a good example of the two-array one. These two groups of indices names and abbreviations are listed with their calculation equation in Tables 5 and 7. These indices are applied to the curves of Fig. 8. The resulted values, along with relevant analysis, are presented in subsections 4.1 and 4.2. These subsections are respectively dedicated to one-array indices and two-array one.

4.1. Evaluation of One-array Indices

One-array indices are introduced in Table 5. For each index, the change percentage of the index value for each of the faulty curves of Fig. 8 relates to the reference curve index value is calculated. Instead of reporting indices' quantities, calculated values are normalized based on the highest amount of the index and plotted versus normalized fault severities to avoid prolongation and have a better comparison.

It means that for each index, the difference of each faulty curve index relative to the reference curve index is divided over the most significant difference to normalize it. Equation (2) shows the formula for normalizing the average index as an example of one-array indices normalization process. In this equation, x is the data array of the reference curve, y is the data array of each faulty curves, and Y is a set of all faulty curves.

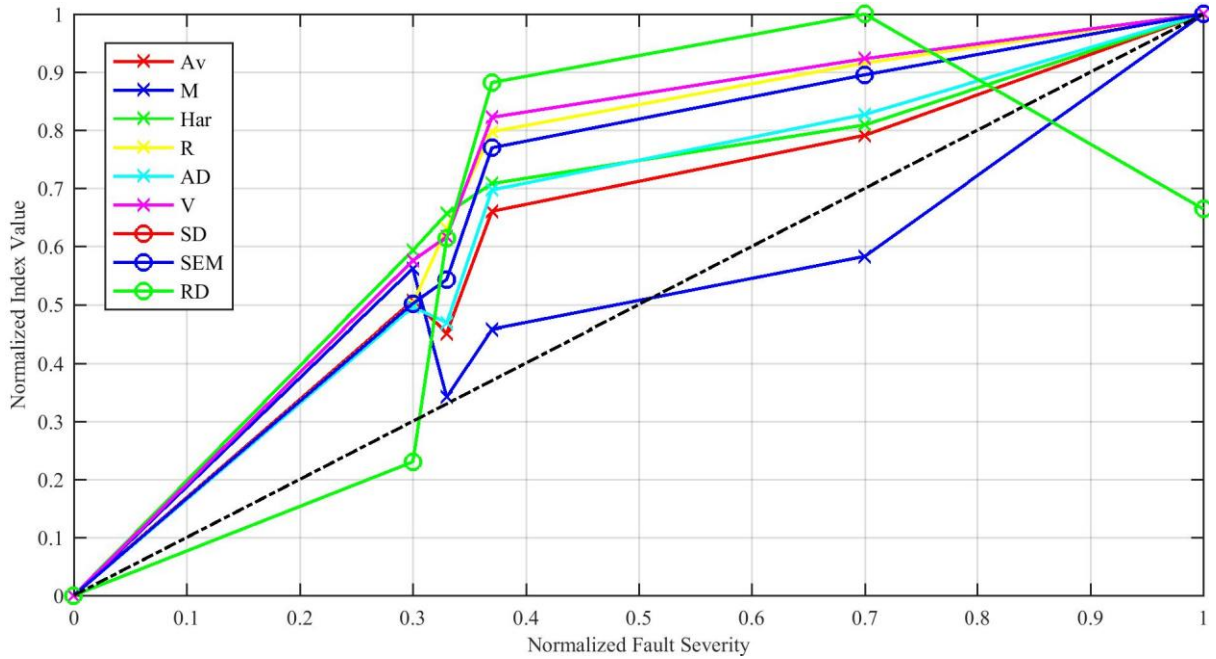
$$Av(y)_{normalized} = \frac{Av(x) - Av(y)}{\max_{y \in Y} [Av(x) - Av(y)]} \quad (2)$$

For normalizing fault severities, the percentage of the short-circuited portion on winding in each fault is split over 50, which is the most severe modeled fault (short-circuit between taps BIII and Ba). Fig. 13 shows the normalized curves of one-array indices.

Table 5: One-array indices

Index	Description
Average (Av)	$Av = \bar{x} = \frac{1}{N} \sum_{i=1}^N x_i$
Median (M)	$M = L + \left(\frac{(N/2) - cf}{f} \right) h$
Harmonic Mean (Har)	$\frac{1}{HAR} = \frac{1}{N} \sum_{i=1}^N 1/x_i$
Range (R)	$R = \max(x) - \min(x)$
Average Deviation (AD)	$AD = \frac{1}{N} \sum_{i=1}^N x_i - \bar{x} $
Variance (V)	$V = \frac{1}{N} \sum_{i=1}^N (x_i - \bar{x})^2$
Standard Deviation (SD)	$SD = \sqrt{\frac{1}{N} \sum_{i=1}^N (x_i - \bar{x})^2}$
Standard Error of Mean (SEM)	$SEM = \frac{SD}{\sqrt{N}}$
Relation Dispersion (RD)	$RD = 100 \left(\frac{SD}{\bar{x}} \right)$

N : Size of the data set
 L : Lower limit of the median class
 cf : Cumulative frequency of classes prior to the median class
 f : Frequency of median class
 h : Median class size
 \bar{x} : Average value of X data set
 x_i : Data points of X data set

**Fig. 13:** Normalized change percentage of one-array indices in different short-circuit fault levels

As the fault becomes more severe, the difference between its curve and the reference curve increases. Although the difference between curves is not constant all over the frequency range, and they may overlap and cross each other in some parts; it is rational to expect that the visible difference between curves due to the fault severity be apparent in the calculated indices too. Therefore, each index curve must have an increment or decrement trend, and checking if an index curve is strictly increasing or decreasing is the first step for evaluating index performance. According to Fig. 13, change percentages of Av , M , AD , and RD indices do not have a strict trend, and in at least one interval, their curve decrease. This issue is considered as a weak point for these indices as they are not able to accurately show the result changes.

The index behavior as the fault severity change is another important topic in the evaluation of indices. In other words, it is remarkable how proportionally index value changes relative to the fault severity change. As it was mentioned, FRA results always change relative to the fault severity, but these changes are not necessarily linear. Hence, completely proportional behavior is not expected in the percentage change of the indices, but the index that changes more proportional to the fault severity change is better, especially for determining fault severity. If neglect the indices that are not strictly increasing in Fig. 13, Har index curve is the closest one to the dotted line (perfectly proportional behavior concerning fault severity changes), and it has the most proportional behavior to fault severity changes.

In addition to the above analyses, the sensitivity and accuracy of the indices are also appraised over the faults that have close severity levels. In Fig. 8, the least severe modeled fault is shown with a green curve and short-circuits 15% of the winding (fault level one). The second severe fault is depicted in purple, which short-circuits 16.5% of the winding (fault level two). The third severe fault (red curve) is two percent more severe than the second one (18.5%) and is called fault level three. The severity levels of these three faults change 1.5%, 2%, and 3.5% relative to each other, which are small numbers.

For each of the indices, the relative two-by-two absolute change percentage of the index values over these three fault levels are calculated. It means that for each index, it is calculated that how much its value for level two fault changes relative to level one; and how much its value changes for level three fault relative to level two fault. Similarly, the change percentage of index value for level three fault relative to level one is measured. The average of these change percentages is presented in Tables 6 as an indicator for the indices' accuracy. The index with a higher average of change percentages has better sensitivity in result comparison.

According to Table 6, the RD index has the most significant value, but it does not have a strictly increasing curve and decreases in the last interval. Subsequently, this index is sensitive and accurate for detecting small faults, but it is not reliable in more massive defects. Among other indices that have approximately the same sensitivity in Table 6, it can be said that the V index is more accurate for fault detection as its percentage difference to the reference value is always larger than others and its curve is above all curves in Fig. 13.

Table 6: Average of two-by-two change percentage of one-array index values for first three fault severity levels

Index	M	Av	Har	R	AD	V	SD	SEM	RD
Average of Two-by-Two Change Percentages	30.56	29.24	12.66	36.99	31.65	27.79	34.51	34.51	164.7

4.2. Evaluation of Two-array Indices

Two-array indices are introduced in Table 7. For evaluating two-array indices, their values are calculated over the curves of Fig. 8, and similar to the previous section, they are normalized and depicted versus normalized values of faults severities. Note that the normalization procedure for these indices is not always the same as one-array ones.

The values of the two-array indices except for CC , COV , MM grow as dissimilarity of compared curves increase. Thus, for normalization, the index value for each curve is divided over the largest one. For instance, the formula for normalizing the $DABS$ index is presented in equation (3). In this equation, x is the data array of the reference curve, y is the data array of each faulty curves, and Y is a set of all faulty curves.

$$DABS(y, x)_{normalized} = \frac{DABS(y, x)}{\max_{y \in Y} [DABS(y, x)]} \quad (3)$$

The CC , COV , and MM indices do not behave like other ones, e.g., CC and MM indices' values are one when two curves are identical, and they get lower as the curves become more different from each other. On the other hand, COV values increase as the curves get more similar to each other. Hence, for normalizing these indices, first, the index is calculated for the sound condition (reference curve is compared with itself, which results in a large number for COV and one for CC and MM). Then, the difference of index values of each faulty curves relative to the index value of sound condition is divided over the biggest difference. Equation (4) normalizes the MM

index as a sample. In this equation, x is the data array of the reference curve, y is the data array of each faulty curves, and Y is a set of all faulty curves.

$$MM(y, x)_{normalized} = \frac{MM(x, x) - MM(y, x)}{\max_{y \in Y} [MM(x, x) - MM(y, x)]} \quad (4)$$

Table 7: Two-array indices

Index	Description
Correlation Coefficient (CC)	$CC = \frac{\sum_{i=1}^N (x_i - \bar{x})(y_i - \bar{y})}{\sqrt{\sum_{i=1}^N (x_i - \bar{x})^2 \sum_{i=1}^N (y_i - \bar{y})^2}}$
Covariance (COV)	$COV = \frac{1}{N} \sum_{i=1}^N (x_i - \bar{x})(y_i - \bar{y})$
Absolute Sum of Logarithmic Error (ASLE)	$ASLE = \frac{\sum_{i=1}^N 20 \log x_i - 20 \log y_i }{N}$
Absolute Average Difference (DABS)	$DABS = \frac{1}{N} \sum_{i=1}^N x_i - y_i $
Min-Max Index (MM)	$MM = \frac{\sum_{i=1}^N \min(x_i, y_i)}{\sum_{i=1}^N \max(x_i, y_i)}$
Sum of Squared Error (SSE)	$SSE = \frac{1}{N} \sum_{i=1}^N (x_i - y_i)^2$
Root of Sum of Squared Error (RSSE)	$RSSE = \sqrt{\frac{1}{N} \sum_{i=1}^N (x_i - y_i)^2}$
Sum of Squared Ratio Error (SSRE)	$SSRE = \frac{1}{N} \sum_{i=1}^N \left(\frac{y_i}{x_i} - 1 \right)^2$
Sum of Squared Max-Min Ratio Error (SSMMRE) [30]	$SSMMRE = \frac{1}{N} \sum_{i=1}^N \left(\frac{\max(x_i, y_i)}{\min(x_i, y_i)} - 1 \right)^2$
Comparative Standard Deviation (CSD)	$CSD = \sqrt{\frac{1}{N} \sum_{i=1}^N [(x_i - \bar{x}) - (y_i - \bar{y})]^2}$
Spectrum Deviation (SpD)	$SpD = \frac{1}{N} \sum_{i=1}^N \sqrt{\left(\frac{x_i}{(x_i + y_i)/2} - 1 \right)^2 + \left(\frac{y_i}{(x_i + y_i)/2} - 1 \right)^2}$
Standardized Difference Area (SDA)	$SDA = \frac{\int_{f_{min}}^{f_{max}} x(f) - y(f) df}{\int_{f_{min}}^{f_{max}} x(f) df}$
Euclidean Distance (ED)	$ED = \sqrt{\sum_{i=1}^N (x_i - y_i)^2}$
N : Size of the data set f : Frequency \bar{x}, \bar{y} : Average value of X and Y data sets x_i, y_i : Data points of X and Y data sets	

Fig. 14 shows the normalized values of two-array indices versus normalized faults severities. The index value of all two-array indices except CC , COV , and MM grows as the compared curves become more apart from each other, and they must have strictly increasing curves. Additionally, although the index value of CC , COV , and MM decreases by fault expansion; due to the described normalization procedure for these three indices, the normalized curves of them must also have an increasing trend. Fig. 14 shows that $ASLE$, $SSRE$, $SSMMRE$, and SpD indices do not have a strict trend, and in some periods, they have misleading values.

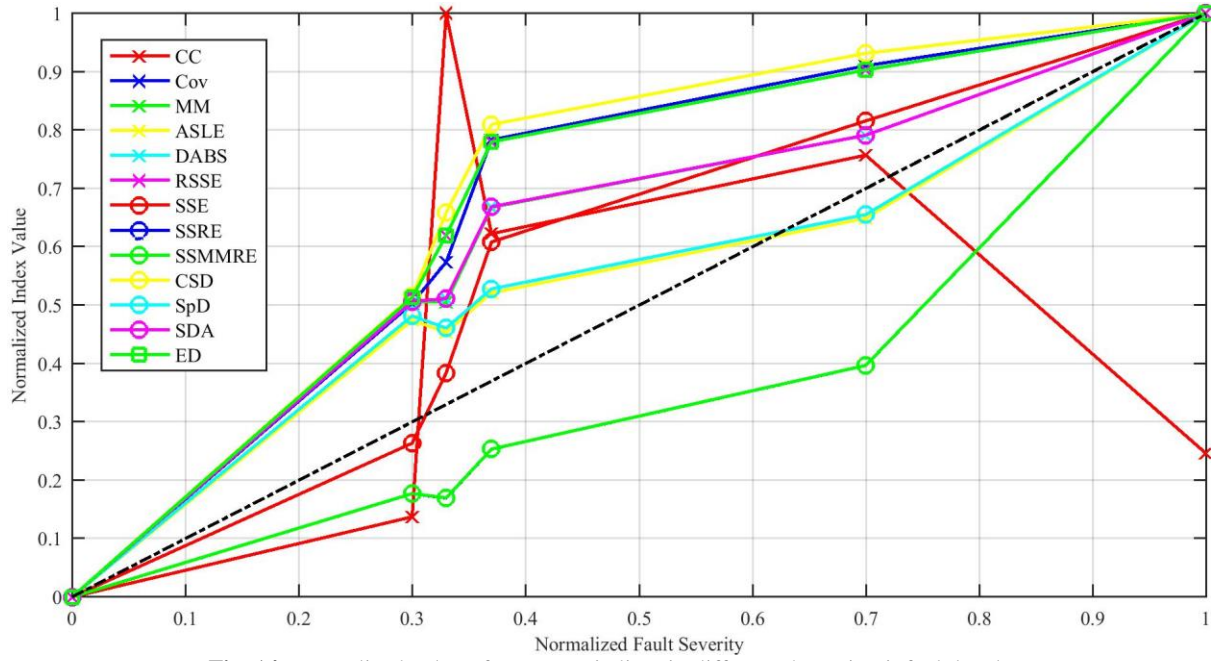


Fig. 14: Normalized value of two-array indices in different short-circuit fault levels

Two-array indices totally change more proportionally to the severity changes than one-array indices, and their curves are closer to the dotted reference line of perfectly proportional behavior. It is apparent in Fig. 14 that *ASLE* and *SpD* have the most proportional behavior to the fault severity changes than all of the one- and two-array indices. It must be noted that these two indices do not have a monotone trend, and it is an issue that must be considered in their application. Among the indices that have monotone trend, *DABS* and *SDA*, which have the same normalized curve in addition to *SSE* are closer to the dotted line and are more linear or behave more proportionally to fault severity changes.

The sensitivity of two-array indices is also analyzed with the same approach as the previous section. Average of two-by-two change percentage of index values are calculated for the first three fault levels and reported in Table 8. Based on this table, *SSE* is the most sensitive index that in average changes about 78 percent for just two percent of fault severity changes. Fig. 14 also shows that *SSE* sharply increases in the first three fault levels, but it does not change like that for more significant fault changes. So, it can be said that *SSE* is useful for small difference detection in the FRA results.

Table 8: Average of two-by-two change percentage of two-array index values for first three fault severity levels

Index	<i>CC</i>	<i>COV</i>	<i>MM</i>	<i>ASLE</i>	<i>DABS</i>	<i>SSE</i>	<i>RSSE</i>
Change Percentage	1.2	11.3	5.5	9.7	21.2	78.3	32.8
Index	<i>SSMMRE</i>	<i>CSD</i>	<i>SpD</i>	<i>SDA</i>	<i>ED</i>	<i>SSRE</i>	
Change Percentage	32.1	35.9	9.5	21.2	32.8	32.2	

4.3. New Index for FRA Studies

The evaluations of the previous section give an overview of the two-array indices application in FRA interpretation and introduce better ones. It also endorses the results of other researches and shows that the *DABS* index has a good performance for FRA interpretation. In addition to the results of the previous section, using *DABS* for evaluation of various curves of this paper showed that this index could reflect the variations in the curves very well. Note that by using this index, the absolute average difference between curves is calculated. This calculated amount of variations between curves is more meaningful if someone considers the range of curve magnitude change. For example, if the FRA curve's magnitude changes from zero to 20 and has *DABS* value of five, and another fault curve's range is 50 but has the same *DABS* value; the former FRA result belongs to a more severe fault as its average difference is a big number in comparison to its range.

Thus, we propose the ratio of *DABS* index to the *R* (Range) of the faulty curve (or any other curve that is compared with reference) as a new index for having better FRA interpretation. This index, which can be called the Absolute Average Difference to Range Ratio (*AADRR*), is calculated by equation (5). Where x is the array of reference curve data points, y is the faulty curve data set, and N is the size of these sets.

$$AADRR = \frac{DABS(x,y)}{R(y)} = \frac{\frac{1}{N} \sum_{i=1}^N |x_i - y_i|}{\max(y) - \min(y)} \quad (5)$$

In order to evaluate the performance of this new index, it is applied to the curves of Fig. 8, and its normalized curve is plotted in Fig. 15. In Fig. 15, the normalized curve of *AADRR* is compared with *DABS* and *SSE*, which are two of the best two-array indices. According to Fig. 15, *AADRR* index has a strictly increasing trend and does not have any problem with following changes of fault levels. Additionally, this index changes more proportional to fault severity than the *DABS* index or any other indices. Note that in almost all of the FRA figures, the range of curves (*R*) decreases as the fault severity increases. So, the *AADRR* index must have more sensitivity than *DABS* index as its denominator decrease when the fault level grows.

To evaluate *AADRR* sensitivity, the average of two-by-two change percentage of this index for the first three fault levels is calculated, and it is equal to 41.8. It is a considerable number and is less than just a few indices. On the whole, the *AADRR* index has excellent performance and can be an alternative for currently in use statistical indices for FRA interpretation.

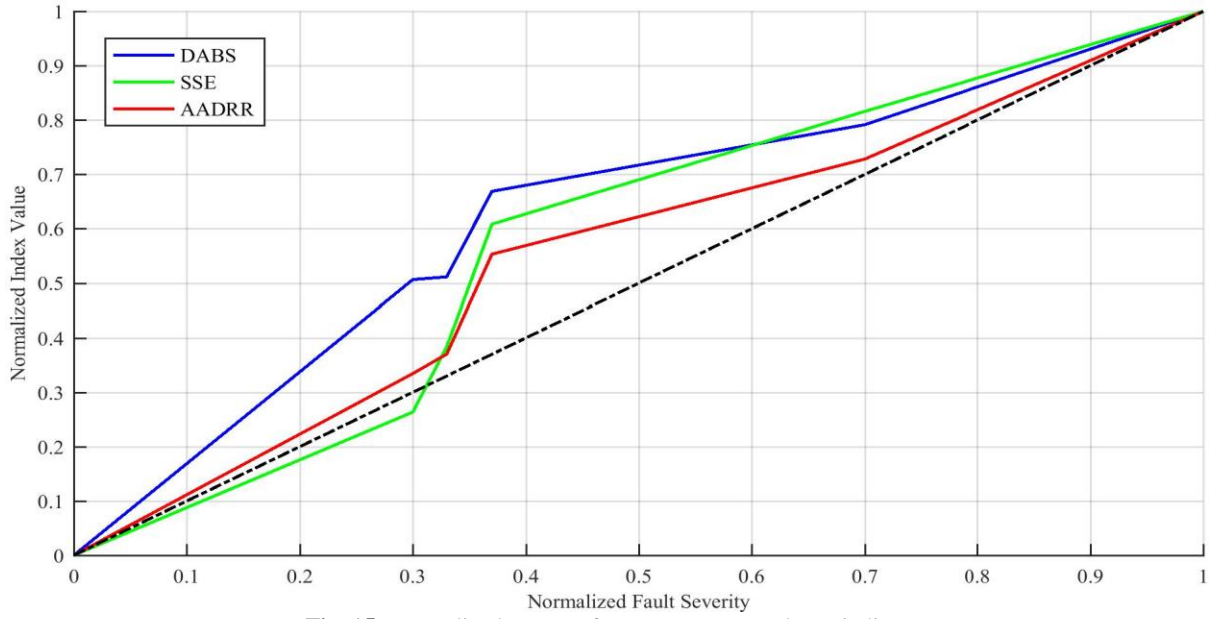


Fig. 15: Normalized curves of *AADRR*, *DABS* and *SSE* indices

5. Conclusion

Frequency response analysis is currently one of the primary fault detection methods in transformers, and its application is growing into the electrical machines field. This paper, which is the first part of a series of papers, addresses some of the fundamental issues related to the applicability and interpretation of FRA in electrical machines by performing experimental tests on a stator of a three-phase wound rotor asynchronous machine. To the best of our knowledge, the FRA test has not been done on this type of machine in previous works.

After ensuring about repeatability of FRA tests and adequacy of the frequency range, it is shown that changes in the rotor's position can affect FRA results of stator even when the rotor is cylindrical. The importance of fixing rotor in the same place for all the tests overtimes is also more emphasized by showing that faults on the stator may reflect differently on FRA results if rotor position changes. Due to the empirical analysis, performing the FRA test on stator when the rotor's terminals are floated (if applicable) is the best circuit configuration for having more accuracy. Additionally, modeling inter-turn and phase to phase short-circuit faults along with insulation weakness on the stator in various severities not only showed the FRA applicability and accuracy for the detection of these failures but also gave a notion of results change pattern due to each fault.

A large number of statistical indices are also analyzed in this work in terms of their accuracy, sensitivity, and proportional behavior considering fault severity changes. The results of these investigations show that *V* (variance) and *RD* (relation dispersion) are the more sensitive one-array indices and *Har* is the one that changes more proportional to fault severity changes. Two-array indices in overall have better performance than one-array ones. Among them, *SSE* (sum of squared error), *SDA* (standardized difference area), and *DABS* (absolute average difference) are more accurate and behave more proportionally to the fault severity changes in comparison to others. This paper proposes a new index for FRA interpretation, which is called absolute average difference to range ratio

(AADRR). Initial analysis showed that it has a remarkably good performance. This index has the potential to significantly enhance FRA interpretation accuracy in either of transformers or electrical machines.

Although this work tried to address most of the fundamental practical issues in the electrical machines' stator FRA, some additional topics like the accuracy of different transfer functions and the effect of ground fault can be studied in future works. Furthermore, as it is an entirely new method for electrical machines, more researches are needed to be done on the interpretation and understanding of FRA results. It is also needed to evaluate the AADRR index performance on other FRA results or even analyzed with more mathematical vision. Finally, developing models for electrical machines based on the results of this work and other similar ones is an ultimate research goal for future works. Using these models, it is possible to more systematically investigate issues in this area, which can result in the standardization of the FRA test for electrical machines. The authors are also working toward this direction.

In order to have a comprehensive study on the topic of electrical machines fault detection through FRA, issues related to rotor fault detection are covered in the later version of this series of papers along with the evaluation of FRA result presenting methods.

Acknowledgment

The authors would like to show their gratitude to Gevork B. Gharehpetian, professor at the Amirkabir University of Technology, Tehran, Iran, for the possibility of performing experiments in his laboratory. Reza Khalili Senobari also wants to thank Ali Asghar Khodadoost Arani for his valuable help in preparing the experimental setup.

References

- [1] S. Nandi, H. A. Toliyat, and X. Li, "Condition Monitoring and Fault Diagnosis of Electrical Motors A Review," *IEEE Transactions on Energy Conversion*, vol. 20, no. 4, pp. 719–729, 2005.
- [2] E. Dick and C. Erven, "Transformer Diagnostic Testing by Frequency Response Analysis," *IEEE Transactions on Power Apparatus and Systems*, vol. PAS-97, no. 6, pp. 2144–2153, 1978.
- [3] R. K. Senobari, J. Sadeh, and H. Borsi, "Frequency Response Analysis (FRA) of Transformers as A Tool for Fault Detection and Location: A Review," *Electric Power Systems Research*, vol. 155, pp. 172–183, 2018.
- [4] M. H. Samimi, S. Tenbohlen, A. A. S. Akmal, and H. Mohseni, "Effect of Different Connection Schemes, Terminating Resistors and Measurement Impedances on the Sensitivity of the FRA Method," *IEEE Transactions on Power Delivery*, vol. 32, no. 4, pp. 1713–1720, 2016.
- [5] M. Bagheri, B. Phung, and T. Blackburn, "Influence of Temperature and Moisture Content on Frequency Response Analysis of Transformer Winding," *IEEE Transactions on Dielectrics and Electrical Insulation*, vol. 21, no. 3, pp. 1393–1404, 2014.
- [6] V. Nurmanova, A. Khassenov, M. Bagheri, T. Phung, and G. Gharehpetian, "The Influence of External Parameters on Transformer Frequency Response Signature and Numerical Indices," in *2019 IEEE International Conference on Environment and Electrical Engineering and 2019 IEEE Industrial and Commercial Power Systems Europe (EEEIC / I&CPS Europe)*, Genova, Italy, 2019.
- [7] K. N. B. Abeywickrama, Y. V. Serdyuk, and S. M. Gubanski, "Exploring Possibilities for Characterization of Power Transformer Insulation by Frequency Response Analysis (FRA)," *IEEE transactions on power delivery*, vol. 21, no. 3, pp. 1375–1382, 2006.
- [8] A. Shamlou, M. R. Feyzi, and V. Behjat, "Interpretation of Frequency Response Analysis of Power Transformer Based on Evidence Theory," *IET Generation, Transmission & Distribution*, vol. 13, no. 17, pp. 3879 – 3887, 2019.
- [9] E. Rahimpour, M. Jabbari, and S. Tenbohlen, "Mathematical Comparison Methods to Assess Transfer Functions of Transformers to Detect Different Types of Mechanical Faults," *IEEE transactions on power delivery*, vol. 25, no. 4, pp. 2544–2555, 2010.
- [10] S. Banaszak and E. Kornatowski, "Evaluation of FRA and VM Measurements Complementarity in the Field Conditions," *IEEE Transactions on Power Delivery*, vol. 31, no. 5, pp. 2123–2130, 2015.
- [11] D. Pham, T. Pham, H. Borsi, and E. Gockenbach, "A New Diagnostic Method to Support Standard Frequency Response Analysis Assessments for Diagnostics of Transformer Winding Mechanical Failures," *IEEE Electrical Insulation Magazine*, vol. 30, no. 2, pp. 34–41, 2014.
- [12] X. Zhao, C. Yao, A. Abu-Siada, and R. Liao, "High Frequency Electric Circuit Modeling for Transformer Frequency Response Analysis Studies," *International Journal of Electrical Power & Energy Systems*, vol. 111, pp. 351–368, 2019.
- [13] M. Bigdeli, M. Vakilian, and E. Rahimpour, "Transformer Winding Faults Classification Based on Transfer Function Analysis by Support Vector Machine," *IET electric power applications*, vol. 6, no. 5, pp. 268–276, 2012.
- [14] A. J. Ghanizadeh and G. Gharehpetian, "ANN and Cross-correlation Based Features for Discrimination Between Electrical and Mechanical Defects and Their Localization in Transformer Winding," *IEEE Transactions on Dielectrics and Electrical Insulation*, vol. 21, no. 5, pp. 2374–2382, 2014.
- [15] O. Aljohani and A. Abu-Siada, "Application of DIP to Detect Power Transformers Axial Displacement and Disk Space Variation Using FRA Polar Plot Signature," *IEEE Transactions on Industrial Informatics*, vol. 13, no. 4, pp. 1794–1805, 2016.
- [16] "Power Transformers - Part 18: Measurement of Frequency Response," IEC 60076-18:2012, 2012.

- [17] "IEEE Guide for the Application and Interpretation of Frequency Response Analysis for Oil-Immersed Transformers," IEEE C57.149-2012, 2012.
- [18] "Technical Brochure no. 342: Mechanical-Condition Assessment of Transformer Windings Using Frequency Response Analysis (FRA)," CIGRE, Tech. Rep., 2008.
- [19] C. Blzquez, F. Blzquez, F. Blnquez, and E. Rebollo, "Application of Sweep Frequency Response Analysis (SFRA) for Inter-turn Detection of in Medium-voltage Coils Manufacturing," CIGRE, Tech. Rep., 2012.
- [20] F. Bl' anquez, C. A. Platero, E. Rebollo, and F. Bl' anquez, "Evaluation of the Applicability of FRA for Inter-turn Fault Detection in Stator Windings," in *2013 9th IEEE International Symposium on Diagnostics for Electric Machines, Power Electronics and Drives (SDEMPED)*, Valencia, Spain, 2013.
- [21] M. Florkowski and J. Furgał, "Detection of Winding Faults In Electrical Machines Using the Frequency Response Analysis Method," *Measurement Science and Technology*, vol. 15, no. 10, p. 2067, 2004.
- [22] M. Florkowski and J. Furgał, "A High-frequency Method for Determining Winding Faults in Transformers and Electrical Machines," *Review of scientific instruments*, vol. 76, no. 11, p. 114701, 2005.
- [23] C. A. Platero, F. Bl' azquez, P. Frias, and D. Ram' irez, "Influence of Rotor Position in FRA Response for Detection of Insulation Failures in Salientpole Synchronous Machines," *IEEE Transactions on Energy Conversion*, vol. 26, no. 2, pp. 671–676, 2011.
- [24] F. Perisse, P. Werynski, and D. Roger, "A New Method for AC Machine Turn Insulation Diagnostic Based on High Frequency Resonances," *IEEE Transactions on Dielectrics and Electrical Insulation*, vol. 14, no. 5, pp. 1308–1315, 2007.
- [25] F. Perisse, P. Werynski, and D. Roger, "High Frequency Behavior of AC Machine: Application of Turn Insulation Aging Diagnostic," in *Conference Record of the 2006 IEEE International Symposium on Electrical Insulation*. Toronto, Ont., Canada, 2006.
- [26] P. Werynski, D. Roger, R. Corton, and J. F. Brudny, "Proposition of A New Method for In-service Monitoring of the Aging of Stator Winding Insulation In AC Motors," *IEEE Transactions on Energy Conversion*, vol. 21, no. 3, pp. 673–681, 2006.
- [27] W. C. SantAna, G. Lambert-Torres, L. E. B. da Silva, E. L. Bonaldi, L. E. d. L. de Oliveira, C. P. Salomon, and J. G. B. da Silva, "Influence of Rotor Position on the Repeatability of Frequency Response Analysis Measurements on Rotating Machines and A Statistical Approach for More Meaningful Diagnostics," *Electric Power Systems Research*, vol. 133, pp. 71–78, 2016.
- [28] F. Bl' anquez, C. Platero, E. Rebollo, and F. Bl' azquez, "Field-winding Fault Detection in Synchronous Machines with Static Excitation through Frequency Response Analysis," *International Journal of Electrical Power & Energy Systems*, vol. 73, pp. 229–239, 2015.
- [29] W. C. SantAna, C. P. Salomon, G. Lambert-Torres, L. E. B. da Silva, E. L. Bonaldi, L. E. d. L. de Oliveira, and J. G. B. da Silva, "A Survey on Statistical Indexes Applied on Frequency Response Analysis of Electric Machinery and A Trend Based Approach for More Reliable Results," *Electric Power Systems Research*, vol. 137, pp. 26–33, 2016.
- [30] J.-W. Kim, B. Park, S. C. Jeong, S. W. Kim, and P. Park, "Fault Diagnosis of A Power Transformer Using an Improved Frequency Response Analysis," *IEEE Transactions on Power Delivery*, vol. 20, no. 1, pp. 169–178, 2005